ELSEVIER SCIENCE

*Tribology International* Vol. 30, No. 2, pp. 129–137, 1997

0301-679X/96/$15.00 +0.00

PII: S0301-679X(96)00036-9

# Rolling contact fatigue performance of detonation gun coated elements

**R. Ahmed and M. Hadfield**

Rolling contact fatigue performance of thermal spray coatings has been investigated using an experimental approach. A modified four ball machine which simulates a rolling element bearing was used to examine the coating performance and failure modes in a conventional steel ball bearing and hybrid ceramic bearing configurations. Tungsten carbide (WC-15%Co) and aluminium oxide ($Al_2O_3$) were thermally sprayed using a super D-Gun (SDG2040) on M-50 bearing steel substrate in the geometrical shape of a cone. A coated cone replaced the upper ball that contacts with three lower balls. The rolling contact fatigue (RCF) tests were performed under immersed lubricated conditions using two different lubricants. Fatigue failure modes were observed using a scanning electron microscope. Microhardness measurements of the coating and the substrate and elasto-hydrodynamic fluid film thickness results are included. The results show the requirement for significant optimization of the coating before use in rolling element bearing applications. The coating was fractured in a delamination mode. Test results show an optimization in coating process is required before these coatings can be used for rolling contact applications. WC-Co coatings perform better than $Al_2O_3$ coatings in rolling contact. Copyright © 1996 Elsevier Science Ltd

**Keywords:** *thermal spray, D-Gun, tungsten carbide, $Al_2O_3$, fatigue*

## Introduction

Thermally sprayed coatings deposited by a variety of processes such as flame, arc wire, detonation gun (D-Gun), and high velocity oxy-fuel (HVOF) etc. are extensively used in the aircraft and automobile industry for resistance against wear, erosion, thermal barrier, oxidation and corrosion etc. Rhys-Jones[1] describes the aero-engine components which are coated to protect against wear, erosion, oxidation and corrosion. Thermally sprayed tungsten carbide cobalt (WC-Co) coatings deposited by D-Gun and HVOF processes are said to provide a high wear resistance. These thermal spraying techniques provide a high particle velocity and moderate temperature during the thermal spraying process. The particle speed during the HVOF process can vary from 150 m/s to 750 m/s, and is typically 600 m/s for the D-Gun process. The gas/particle temperature during a HVOF process varies from 1400°C to 2000°C, whereas for the D-Gun process it is in excess of 3000°C. Plasma spraying processes generate gas/particle temperatures in the excess of 16 000°C.

The advancements in the thermal spraying techniques can be utilized by investigating new applications. This study addresses the rolling contact fatigue (RCF) performance of WC-Co and alumina ($Al_2O_3$) coatings deposited by the D-Gun (SDG 2040) process. The performance and failure mode of these coatings can thus provide a feedback for the optimization of these coatings. The brittleness and weakness of sprayed coatings is due to the lamella structure of sprayed coatings, where individual lamellas are said not to adhere to one another completely. Thus these coatings at present are limited to low contact stress applications[2]. Research

*Brunel University, Department of Mechanical Engineering, Uxbridge, Middlesex UB8 3PH, UK*
*Received 19 June 1995; revised 26 January 1996; accepted 24 April 1996*

is thus required to investigate the performance and failure mechanism of thermal spray coatings to enable their use in advanced contact applications. Advanced materials like ceramics are beginning to replace steel in rolling contact bearings for particular applications like aero-engines[3] and high speed machine tools[4]. It may be possible to reach the full potential of hybrid ceramic bearings and increase the performance of bearing steels by using thermal spray coatings, e.g. in raceway applications. In this way thermal matching between coated and parent components may be optimized. An advantage of this coating method is its compatibility with mass production techniques.

## Some previous studies

Previous studies on the RCF performance of thermal spray coatings are limited. Initial studies by Tobe *et al.*[5] on the RCF behaviour of thermal sprayed ceramic and metallic coatings showed that ceramic coatings of convex surfaces show higher rolling fatigue strength than metallic coatings. Their later studies[6] on plasma sprayed coatings showed that the delamination behaviour of some ceramic coatings was preceded by the generation of a blister. They reported that the compressive strength of the coating and shear strength between coated layer and substrate are the most important factors for RCF performance. Keshavam *et al.*[7] in their study reported that the D-Gun coating technique can be used in improving the life of thrust bearings in drilling applications. However, a delamination behaviour of the WC-Co coatings was observed for radial bearing sleeves. Makela *et al.*[8] during their preliminary study on the RCF performance of WC-Co coatings reported that the tribological conditions can effect the micro pitting and delamination of these coatings. Hadfield *et al.*[9] reported that the failure mode of some thermal spray coatings in rolling contact applications is delamination. They observed that WC-Co coatings were delaminating from within the coating microstructure, while aluminium oxide coatings were failing at the interface of coating and substrate. This fact could be attributed to the restricted melting of the oxides during the thermal spraying process.

There has been limited research in the RCF application of thermal spray coatings; extensive data are available on the RCF performance of other coating techniques, e.g. physical vapour deposition (PVD) etc. Although the microstructure, film thickness and physical properties of these PVD coatings differ from thermal spray coatings, their RCF study shows that the substrate hardness and coating thickness are critical to their performance. These factors can also be critical to the RCF performance of thermal spray coatings. In general coating properties like hardness, thickness, surface finish, porosity, adhesive strength, residual stress and the substrate suitability along with the tribological environments prevailing during the rolling contact are critical to the performance of a coating in rolling contact. A balance among these properties can thus help in optimizing the performance of the coating.

## Experimental procedure

### Test configuration

A modified four-ball machine shown as Fig 1 was used to test the coated cone elements. This machine provides an accelerated method to compare the rolling contact fatigue resistance of materials under various tribological conditions.

The assembly was loaded via a piston below the steel cup from a lever-arm load. The coated cone was assembled to a drive shaft via a collet. The cone contacts with the three lower balls after a load is applied. The lower balls are free to rotate. The contacting surfaces between the coated cone and lower balls were immersed in lubricating oil. The coated cone angle which influences the surface roll/slip ratio was fixed at 45°.

A heater beneath the cup can be used to control lubricating oil bulk at elevated temperatures. Spindle speed may be varied up to 20000 rpm from high or low speed drives. Test time and spindle revolutions were recorded by a timer and tachometer. The machine may be set to stop either at revolution number or a maximum vibration amplitude. A thermocouple immersed in the lubricant was used to measure the oil bulk temperature for the tribological conditions of testing.

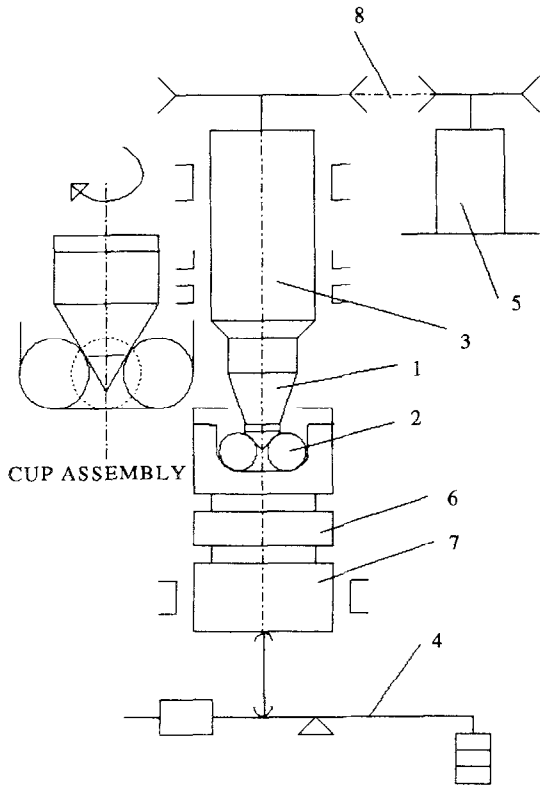


*Fig 1 Schematic of the modified four-ball machine: 1, coated cone and collet; 2, lower balls; 3, spindle; 4, loading lever; 5, driving motor; 6, heated plate; 7, loading piston; 8, belt drive*

### Coated cone test elements

Detonation gun sprayed tungsten carbide coatings are well known for their extremely high resistance against sliding wear, abrasion and fretting[10]. A high impact kinetic energy of coating particles is utilized using a super D-Gun (SDG 2040) to spray two different types of coatings. Tungsten carbide (WC-15%Co) and aluminium oxide ($Al_2O_3$) are sprayed on M-50 bearing steel substrate. Properties such as hardness, corrosion resistance, wear resistance, and adhesive strength are the major attractions in the selection of these coating materials. The selection of substrate material as M-50 steel is based on its high tempering temperature and good combination of toughness/hardness for rolling contact fatigue applications.

The substrate shape for the test pieces during this study was a 14.5 mm diameter cone with an apex angle of 90°. The substrate is sand blasted prior to the coating process to assist strong mechanical bonding between the coating and substrate. Table 1 describes some of the physical properties of the two coating materials obtained from the coating supplier data sheet. Physical properties of thermal spray coatings like modulus of elasticity, Poisson's ratio, adhesive strength etc. vary significantly not only by changing the parameters controlled during the coating process but also with the method of measurement. Hence the listed values are used to provide an estimate of these physical properties.

### Lower ball contacting elements

The selection of lower balls contacting elements which serve the purpose of rolling elements in any rolling bearing was based on the simulation of a traditional steel ball bearing and also a hybrid ceramic bearing. Thus the two materials used for the lower balls contact elements are bearing steel and silicon nitride ceramic. The steel lower balls were 12.7 mm diameter, grade 10 (ISO 3290-1975) carbon chromium steel with an average surface roughness (*Ra*) of 0.02 μm and hardness of 64 HRC. The silicon nitride is manufactured by the hot isostatically pressed (HIP) method supplied by UBE Limited. Ball blanks were ground and polished to a 12.7 mm diameter, and standardized procedures were adopted to ensure consistent quality of material and geometry. The average roughness (*Ra*) of ceramic ball surface was 0.01 μm and the ball roundness was within standard ball bearing tolerances.

The cup used to hold the planetary balls serving the purpose of the outer race of rolling contact bearing was designed to simulate type-II[11] contact conditions between the cup and the planetary balls. The cup material used was bearing steel and the hardness of the cup was 65 HRC.

**Table 1 Physical properties of test coatings**

| | Tungsten carbide (WC-15Co) | Aluminium oxide ($Al_2O_3$) |
|---|---|---|
| Hardness Hv300 (kg/mm²) | 1150 | 1000 |
| Adhesive strength (kg/mm²) | 7.0 | 6.3 |
| Porosity (%) | 1.0 (max.) | 2.0 (max.) |
| Young's modulus (kg/mm²) | 22500 | 9800 |
| Coefficient of thermal expansion (1/C°) | $8.5 \times 10^{-6}$ | $6.7 \times 10^{-6}$ |

### Sample preparation

The test cones were sprayed to an initial thickness of 100 μm and were ground and polished to achieve an average coating thickness of 70 μm. The thickness of the coatings was verified using a high magnification microscope. In this method the tip of the cone was ground off by approximately 300 μm and then examined to measure the radius of the two concentric circles. Fig 2 represents a typical result. Basic trigonometric relations were then used to calculate the thickness of the coating. Owing to the porosity and anisotropy of the sprayed coated material the final surface finish achieved on these samples using conventional methods was 0.04 μm to 0.05 μm Ra. These surface roughness values were taken using a Talysurf series with step motor transfer table from Rank Taylor Hobson Ltd. The cutoff used was 0.25 mm with a Gaussian type filter.

### Micro-hardness measurements

A Leitz miniload 2, Vickers, knoop and scratch hardness tester was used to measure the micro-hardness of the coating and substrate at different geometrical locations. The surface exposed after grinding the tip of the cone (for thickness measurements) is utilized for these measurements. The surface is polished using diamond paste to attain a smooth flat surface and etched in general purpose austenitic nickel and stainless steel etchant to provide a contrast between the coating and the substrate. Preliminary measurements on the micro hardness of test pieces using a variety of loads ranging from 50 p to 400 p, revealed that a load of

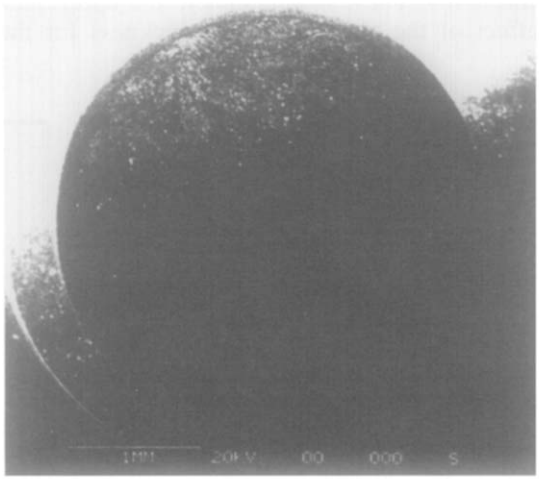

*Fig 2 Coating thickness*

100 p for the substrate and 300 p for both the coating types provide consistent results. Twenty measurements on a typical cone reveal an average microhardness of the WC-Co coating as 1200 Hv and $Al_2O_3$ coating as 1050 Hv, whereas the substrate hardness was 658 Hv. These values are averaged after neglecting the maximum and minimum reading values. The location of these hardness measurements can be appreciated from Fig 3. The major objective of this analysis was to investigate the variation in hardness of the coating and the substrate. The tests revealed that the hardness of the coating varies from 1100 Hv to 1300 Hv, while that of the substrate varies from 625 Hv to 725 Hv. Microhardness tests on the planetary steel balls at 100 p load showed an average microhardness of 850 Hv.

## Test conditions

Two lubricants are considered for the testing program. B.P. Hitec 174 is a high viscosity paraffin hydrocarbon lubricant which has a kinematic viscosity of 200 c.s.°C at 40°C and 40 c.s.°C at 100°C. This lubricant is not commercially available. Exxon 2389 is a synthetic lubricant which has a kinematic viscosity of 12.5 c.s.°C at 40°C and 3.2 c.s.°C at 100°C. Tests were conducted at 1450 rpm with 185 N applied to the cup assembly. The elastohydrodynamic lubrication (EHL) minimum film thickness calculations for these lubricants were made using the following relation by Hamrock and Dowson[12]:

$$H_{min} = 3.63\ U^{0.68}\ G^{0.49}\ W^{-0.073}\ (1-e^{-0.68k}) \qquad (1)$$

where $H_{min}$ is the minimum film thickness, $U$ is the dimensionless speed parameter, $G$ is the dimensionless materials parameter, $W$ is the dimensionless load parameter and $k$ is the dimensionless ellipticity parameter. Figure 4 represents the EHL calculation results for the test conditions for the two lubricants. Results indicate a high value of film thickness for Hitec-174 lubricant which is mainly due to its high dynamic viscosity. Analysis also revealed that there is less than 3% change in the value of $H_{min}$ if the data for the Young's modulus and Poisson's ratio of the test cone are changed from steel to the coating material.

The results are shown in terms of contact configuration and a ratio of the minimum film thickness to average roughness ($\lambda$). These results enable the appreciation of the effect of the change in film thickness for the test

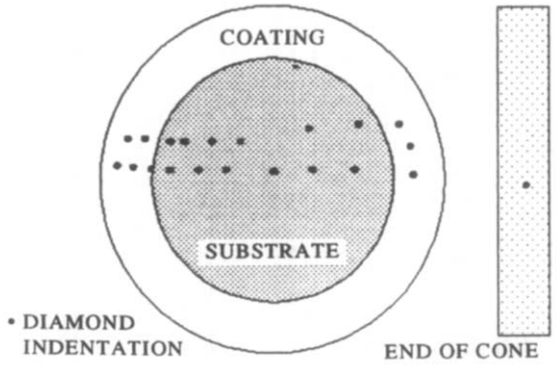


*Fig 3 Location of micro-hardness measurements*

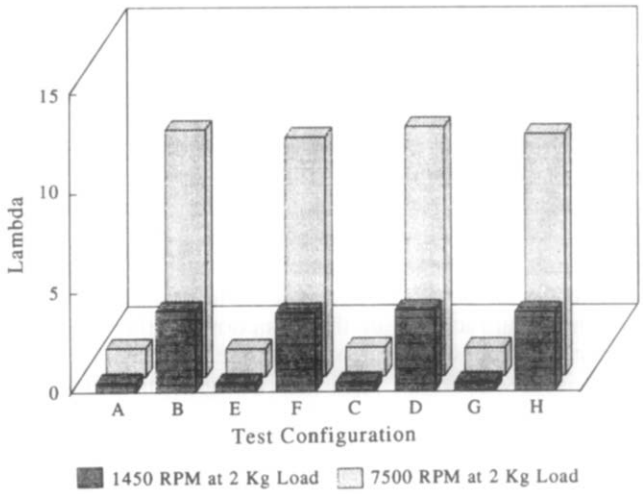


*Fig 4 EHL results. Ra (balls) 0.012 μm; Ra (cone) 0.05 μm (A: WC\Steel\Exxon2389; B: WC\Steel\Hitec174; C: $Al_2O_3$\Steel\Exxon2389; D: $Al_2O_3$\Steel\Exxon2389; E: WC\Ceramic\Exxon2389; F: WC\Ceramic\Hitec174; G: $Al_2O_3$\Ceramic\Exxon2389; H: $Al_2O_3$\Ceramic\Hitec174)*

conditions and their effect on the fatigue life. The results indicate that the lubrication conditions for the test conditions vary from boundary to fully developed elastohydrodynamic film.

Hertz contact stress for the uncoated test cone in contact with the planetary balls at 2 kg lever arm load shows the results given in Table 2. Here $a$ and $b$ represent the radii of the major and minor dimensions of the contact ellipse. The analysis of coated test cones has not been included and requires modelling. The depth of maximum shear stress is approximately the same as the coating thickness. This depth will vary in the presence of friction and due to the difference in Young's modulus and Poisson's ratio of the coating and the substrate.

## Results and surface observations

### Test results

Figure 5 represents the test RCF results at 2 kg lever arm load and 1450 rpm, in terms of the contact configuration, lubricant and the time to failure. The test results are not intended for use as a basis for statistical fatigue life prediction, but as an indication of the coating performance and failure mode in various tribological conditions. The RCF tests at 7500 rpm did not last more than three minutes and are not included in Fig 5.

The first observation from Fig 5 is that the coated cones do not perform well in terms of durability or time to failure. Tests with uncoated M50 steel cones under the same conditions were suspended without failure after surpassing the coated cone cycles to failure. Secondly, the tungsten carbide coated cones generally performed better than the aluminium oxide in all test configurations.

**Table 2**

| Planetary balls | Contact load (N) | Contact dimension *a* (mm) | Contact dimension *b* (mm) | Maximum compressive stress (GPa) | Maximum shear stress (GPa) | Depth of maximum shear (μm) |
|---|---|---|---|---|---|---|
| Steel | 185 | 0.238 | 0.122 | 3.0 | 0.9 | 75 |
| Ceramic | 185 | 0.224 | 0.115 | 3.4 | 1.1 | 71 |

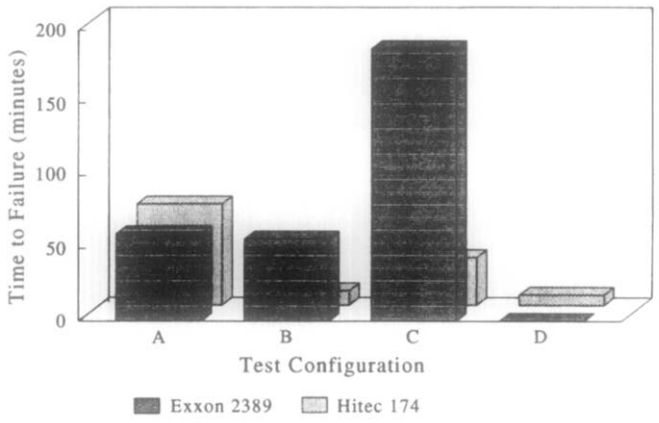


*Fig 5 Rolling contact fatigue test results. A: WC\steel; B: $Al_2O_3$\steel; C: WC\ceramic; D: $Al_2O_3$\ceramic*

The third observation from these results is that the coated cones in contact with steel lower balls generally compare well with the results from contact with ceramic lower balls. This fact may be due to the higher contact stress of ceramic material due to the increase of elastic modulus, i.e. 207 GPa (steel) to 310 GPa (silicon nitride), as well as the increased hardness of ceramic balls. One surprising result is the tungsten carbide coated cone in contact with silicon nitride lower balls lubricated with Exxon 2389. In this case the time to failure reaches over 180 min.

## Surface observations

Figure 6 shows scanning electron microscope (SEM) observations of a failed tungsten carbide coated cone. In this case the coated cone was tested in Exxon 2389 lubricant in contact with steel lower balls. Figure 6a shows the overall failed area and the failure mode of severe delamination. It is important to note that there is no significant wear track on the periphery of the cone, i.e. the specimen failed before any significant wear track was formed. It indicates that the failure of the coating was much more dependent on sub-surface effects rather than surface effects. The width of the delamination was approximately 1.5 mm. It is interesting to see edge cracks 1 mm to the left of the delamination area (Figs 6b–6d). Furthermore, the edge cracks are on the edge of the wear track which is near to the cone apex angle, i.e. the edge subjected to higher contact stress. Edge cracks have been observed before on ceramic materials during rolling contact fatigue tests[13]. These edge cracks may initiate fatigue failure and are thought to be caused by tensile stresses located at the contact surface edge. In the case of the aluminium oxide coatings there was no evidence of edge cracks on the surface.

Figure 7 shows the delamination failed tungsten carbide cone rotated to view the delamination cliff edges. The image in Fig 7a shows the cliff edge towards the rolling direction where a crack at the base is evident. Here the failure depth is approximately 40 μm compared with a mean coating thickness of 75 μm. This implies that the fatigue failure occurs within the tungsten carbide coating and not de-bonding from the substrate. EPMA chemical analysis of the exposed delamination failure also suggested de-bonding through the coating itself. In the case of aluminium oxide failures in coating itself de-bonded from the metal substrate. The image in Fig 7b shows the failure initiation from the rolling direction. Here the delamination failure depth is significantly reduced.

A typical flake-like wear debris is shown in Fig 8. It can be seen that the dimensions of this debris are approximately $1.2 \times 0.6$ mm. The tope edge in Fig 8a shows that the smooth polished surface is relatively intact. The underside of the debris (Fig 8b) shows the surface of the delaminated surface.

Figure 9 represents the SEM micrographs typical results for ceramic coating. In these tests, the coating delaminated from the substrate. This is confirmed by EPMA analysis. A section of coating was also studied which revealed the same result. Figure 9a shows the overall failed area, whereas Fig 9b gives some details of the failed area.

## Residual stress

Spalling and cracking of the coating could have been due to high residual stresses in the coatings. Hence an attempt to measure the residual stress of the test cones was made using an X-ray-diffraction technique. Although the measurement depth using this process is not large the process was selected because of its ability to measure complex sample shapes and also because the process is non-destructive. The $\sin^2\psi$ method which measures the crystal inter-atomic distance was employed. A detailed explanation of this method is given by Farrahi *et al.*[14]. The failed tested cones did not give statisfactory residual stress measurement results due to small diffraction peaks even after several repeated attempts. It was postulated that either the crystallization of the D-Gun coatings was not good, or the grain size was not large, which can be due to the parameters controlled during the thermal spraying process. It is probable that the coating material changed

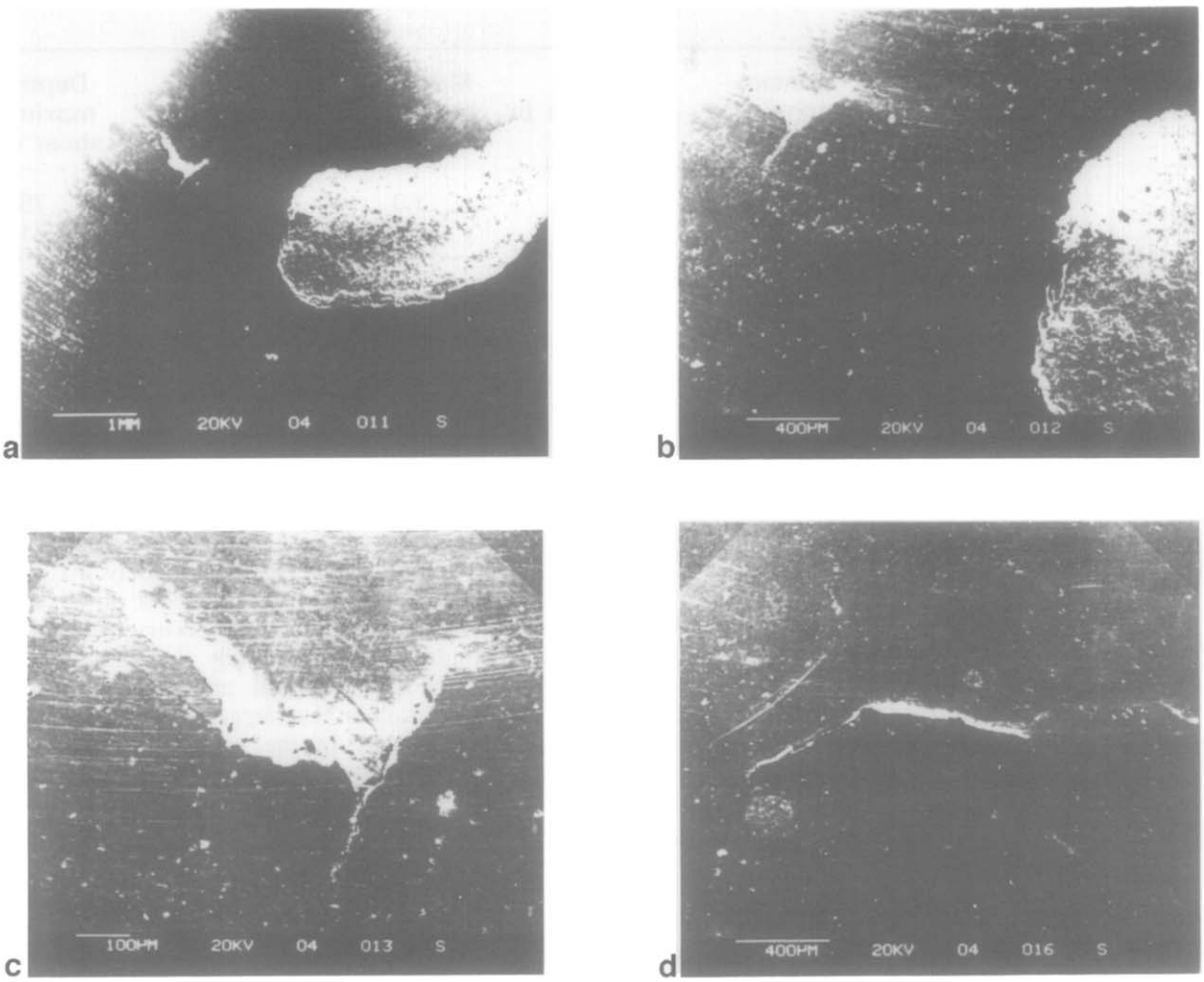


*Fig 6 Observations – tungsten carbide/steel contact (Exxon 2389 lubricant): (a) overview of failed area; (b) edge cracks; (c) edge crack detail; (d) edge crack end*

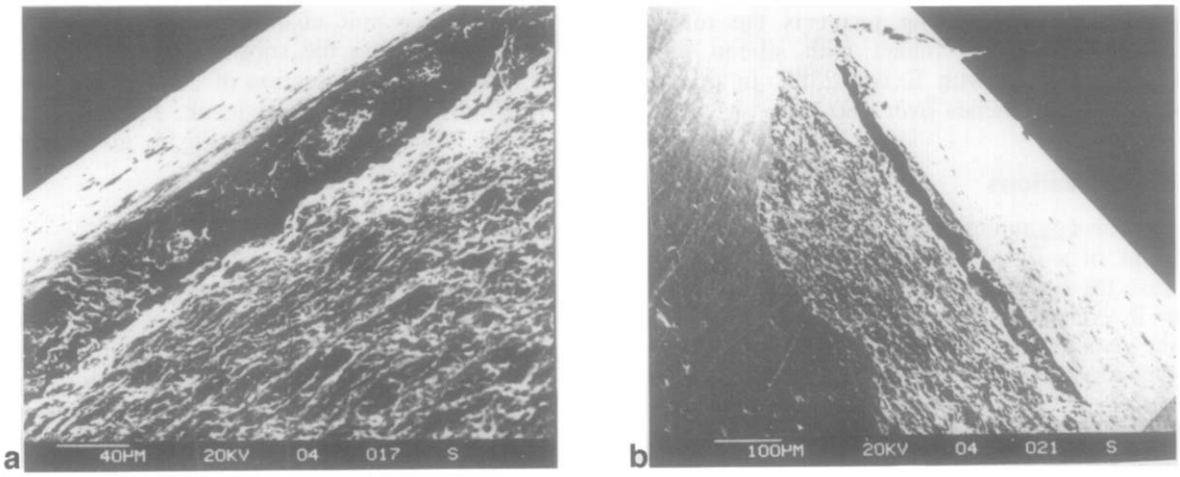


*Fig 7 Delaminated edge – tungsten carbide/steel contact (Exxon 2389 lubricant): (a) cliff edge; (b) cliff edge – initiation*

to a non-crystal material due to the quick cooling in the thermal spray process.

## Discussion

The extent of retained WC in a Co matrix generally represents the wear resistance of WC coatings. This is dependent upon the spraying method and the parameters during the spraying e.g. particle size, type of powder used, velocity of spray, surrounding atmosphere and the substrate temperature. Cryogeneic fracture study of plasma sprayed WC coatings by George *et al.*[15] revealed that these coatings not only have significant porosity but also secondary phase particles and

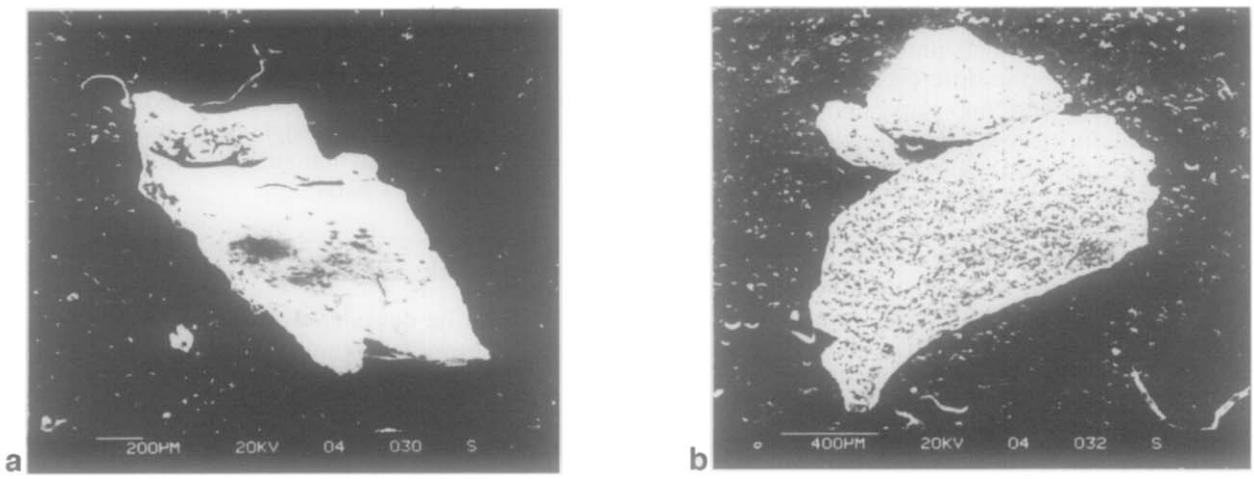


*Fig 8 Debris – tungsten carbide/ceramic contact (HiTec 174 lubricant): (a) debris (top surface); (b) failure surface*

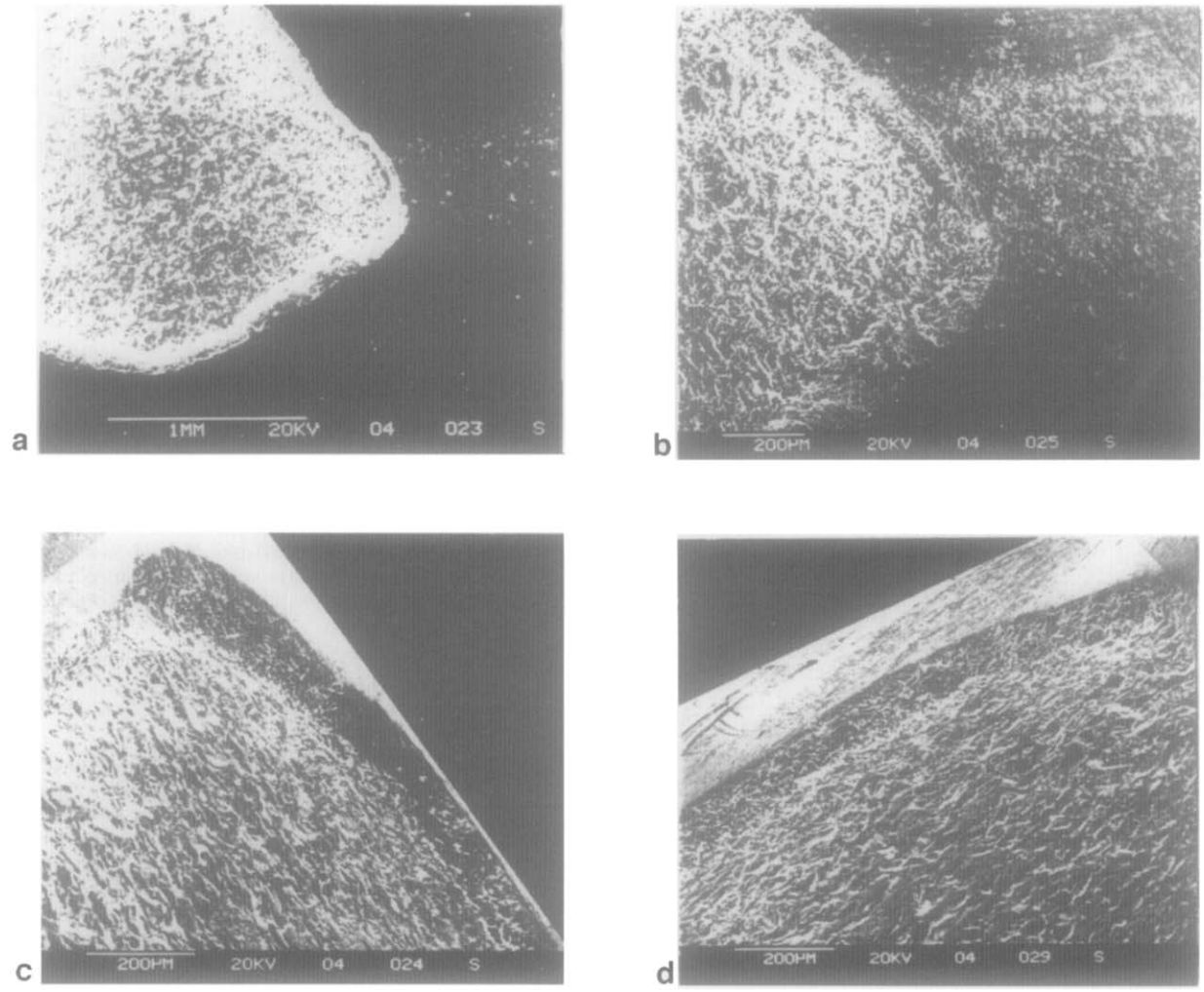


*Fig 9 Observations – aluminium oxide/steel contact (Hitec 174 lubricant): (a) overview of failed area; (b) delamination failure; (c) failed area; (b) delamination failure*

lack of fusion. Vuoristo *et al.*[10] have shown that there is a dominant change in coating microstructure, i.e. improved quantity of retained WC, if coarser coating powders are used. Also, finer powders result in undesirable coating phases but have the advantage of low porosity levels. The delamination failure of these coatings can be thought to be as a result of these porosity/microcracks and secondary phases, i.e. voids due to a plastic flow of matrix around hard particles. Kersharam *et al.*[7] have also reported a delamination behaviour of the WC-Co coatings by D-Gun in a test configuration for radial and thrust bearings. Another

reason for the delamination of the coatings could be the shift in the depth of maximum shear stress at the depth of failure due to the difference in elastic properties of the coating and the substrate. This analysis requires a three-dimensional modelling of the contact configuration for the two types of coated samples in contact with steel and ceramic balls, and has not been attempted during this study. The rolling friction can also alter the maximum shear stress depth; although no measurements were made to specifically measure the value of rolling friction for these coatings, previous studies have shown that the value of rolling friction is very low. The role of residual stress can also be significant.

It is interesting that the λ-value is higher for the tests with Talpa-20 lubricant, but the average time to failure is less. Although the reason for this is not yet verified, it can be thought to be as a result of either a chemical reaction between the coating and lubricant or a hydrostatic pressure build-up due to fluid entrapment.

The micro-hardness measurements showed a variation in the Vickers hardness throughout the coating section. This is in accordance with the analysis presented by Lin[16]. The micro-hardness tests on the planetary balls indicate that the average micro-hardness of the substrate was approximately 200 Hv lower than that of the standard bearing steel used for the planetary balls. It can actually degrade the performance of the coating by not supporting the coating, since the performance of the coating is a combination of coating and substrate.

The $Al_2O_3$ coatings where the failure is at the interface specifically suffer from thermal and mechanical mismatch between the coating and substrate. This difference seems less intense for WC-Co coatings where the failure is not at the interface. The $Al_2O_3$ fails due to the poor adhesive strength whereas in the case of WC-Co coatings the cohesive strength of the coatings needs improvement. Since the difference in coefficient of thermal expansion between the substrate and the coating is larger for $Al_2O_3$ coatings in comparison to WC-Co coatings the residual stress build-up at the interface can be large for $Al_2O_3$ coatings. The increase in coating thickness can cause the maximum principal shear stress to move towards the interface and coating can fail by peeling from the substrate. A solution could be to use either HIP method or heat treatment, although other coating methods like HVOF can also be investigated.

The coatings also suffer from low shearing strength, since in the tests conducted at high speeds of 7500 rpm the coatings' time to failure was less than a minute for a contact stress of 5.8 GPa. The failure mode remained as delamination.

## Conclusions

Tungsten carbide coatings performed better, in rolling contact fatigue resistance, than aluminium oxide under the specific test conditions.

Edge cracks which may have initiated fatigue failure were observed on tungsten carbide surfaces but not on aluminium oxide test cones. Delamination occurred through the coating itself for tungsten carbide. Failure of aluminium oxide occurred by the coating de-bonding from the metallic substrate.

Micro hardness measurements revealed that the coating microhardness varies throughout its section. Moreover, the microhardness of the substrate is less than that of the planetary steel balls.

## Future work

Results can be considered preliminary, and suggest an approach towards optimization of appropriate coating processes and controlling the process parameters. Analysis of the contact stresses within the coated samples during rolling contact and the generation of residual stresses in the coatings need further investigation. Post treatment of the coatings like HIP and heat treatment might show different results.

## Acknowledgements

The authors would like to acknowledge Professor Shogo Tobe of Ashikaga Institute of Technology, Japan, for his help in the preparation of coatings. The authors also acknowledge the financial support by the Overseas Research Scholarship Scheme which is partly funding this research project.

## References

1. **Rhys-Jones T.N.** The use of thermally sprayed coatings for compressor and turbine applications in Aero-engines. *Surf. Coat. Technol. 1990,* **42,** *1–11*
2. **Mcpherson R.** The structure and properties of plasma sprayed alumina coatings. *Alumina conference, Prague, August, 1990*
3. **Hamburg G., Cowley P. and Valori R.** Operation of an All-Ceramic mainshaft roller bearing in a J-402 gas-turbine engine. *J. ASLE, Lubr. Eng. July. (1980) 407–415*
4. **Aramaki H., Shoda Y., Morishita Y. and Sawamoto T.** The performance of ball bearings with silicon-nitride ceramic balls in high speed spindles for machine tools. *J. Tribol. 1988,* **110,** *693–698*
5. **Tobe S., Kodama S. and Sekiguchi K.** Rolling fatigue behaviour of plasma coated steel. *Proc. Surface Engineering Int. Conf., Japan Thermal Spraying Society, Tokyo, Japan October 1988, 35–44*
6. **Tobe S., Kodama S. and Misawa H.** Rolling fatigue behaviour of plasma sprayed coatings on aluminium alloy. *Thermal Spray Research and Applications, Conference Proc. ASM International, OH 1991, 171–178*
7. **Keshavan M.K. and Kembaiyan K.T.** Wear characterization and practical applications of thermal spray coatings in drilling applications. *Conf. Proc. National Thermal Spray Conference, Anaheim, CA, ASM International, OH, USA, 1993, 635–641*
8. **Makela A., Vouristo P., Lahdensuo M., Niemi K. and Mantyla T.** Rolling contact fatigue testing of thermally sprayed coatings. *Thermal Spray Industrial Applications, Conf. Proc. ASM International, OH, USA, 1994, 759–764*
9. **Hadfield M., Ahmed R. and Tobe S.** Rolling contact fatigue of thermally spray coated cones. *Int. Thermal Spray Conf. Kobe, Japan, Thermal Spraying Society, Tokyo, Japan, May 1995, 1097–1102*
10. **Vuoristo P., Niemi K., Makela A. and Mantyla T.** Spray parameter effects on structure and wear properties of detonation gun sprayed WC + 17% Co coatings. *Conf. Proc. National Thermal Spray Conference, Anaheim, CA, ASM International, OH, USA, 1993, 173–178*

11. **Tourret R. and Wright E.P.** Rolling contact fatigue: performance testing of lubricants. *Int. Symp., I. Petroleum, October 1976, Heyden & Son, London, 1977*

12. **Jacobson B.O.** Rheology and Elastohydrodynamic Lubrication. Baker and Taylor, *1991*

13. **Lucek J.W.** Rolling wear of silicon nitride bearing materials. *ASME, 90-GT-165, Gas Turbine and Aero-Engine Congress and Exposition, June 11–14, Brussels, Belgium, 1990*

14. **Farrahi G.H., Markho P.H. and Maeder G.** A study of fretting wear with particular reference to measurement of residual stresses. *Wear 1991,* **148,** *249–260*

15. **George F. and Voort V.** A layman's view of plasma spray coating metallography. *Structure, 1995, 8–13*

16. **Liń C.K. and Berndt C.C.** Microhardness variations in thermally sprayed coatings. *Conf. Proc. National Thermal Spray Conference, Anaheim, CA, ASM International, OH, USA, 1993, 561–568*